

MASS simulations under strong scintillation

A. Tokovinin

Version 4. February 8, 2006
file: prj/atm/mass/theory/doc/simul06.tex

1 Method

Continuing the study of MASS behavior under string scintillation, we simulated intensity patterns resulting from a single turbulent layer, of varying intensity. The turbulence strength is parametrized by the seeing (at 500nm).

The code `simatmpoly.pro` computes intensity distributions for polychromatic light passing through an arbitrary number of turbulent phase screens. The turbulence profile is specified by the relative strength of these screens (sum to unity), the total is determined by the seeing. The polychromatic light is modeled by a set of discrete wavelengths $[\lambda]$, each with its own intensity $[sp]$. Each wavelength is propagated (independently of others) through the common set of screens, and the resulting intensity patterns are averaged with the relative weight $[sp]$.

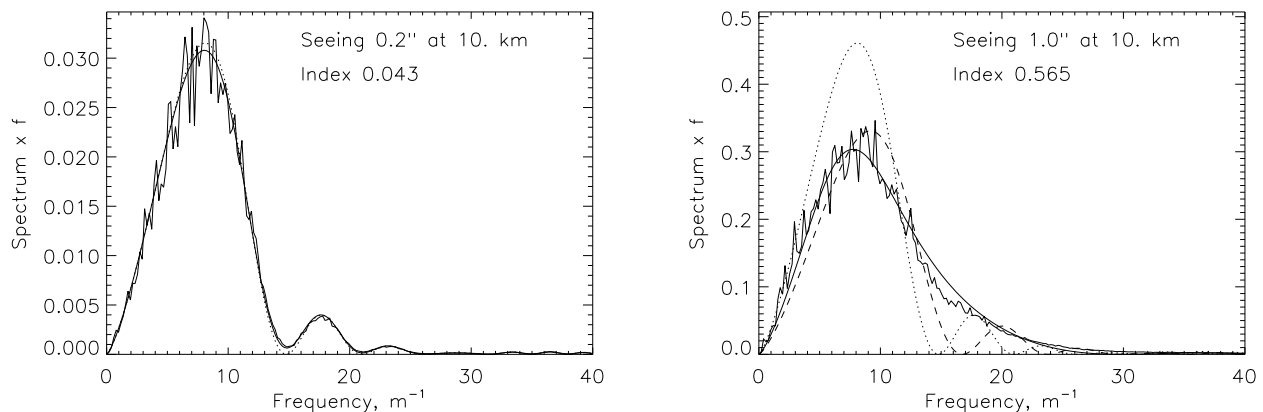


Figure 1: Simulated and modeled power spectra of poly-chromatic scintillation. Left: 0.2" seeing at 10km, right – 1" seeing at 10km. The wavelengths of 0.4, 0.55, and 0.5 μm are mixed with equal weight. The dotted curves are weak-scintillation models, the full curves – new models, and the dashed curve on the right-hand plot shows the weak model with reduced layer height.

Tests (Fig. 1) have shown that the spatial spectra of these intensity patterns match very well the results of poly-chromatic scintillation theory, in case of weak scintillation (code `intsp7a.pro`). As scintillations become stronger, the energy is transferred from low frequencies to higher frequencies and “fills in” the gaps in the spatial power spectrum due to Fresnel propagation. This behavior is

qualitatively similar to the monochromatic case, except that the high-frequency component decreases faster, just as in the case of weak scintillation.

Interestingly, for $1''$ seeing the low-frequency part of the spectrum is well represented by the classical weak-scintillation model with a scaled (reduced) height, the scaling being $1 + 0.5\sigma_I^2$ (dashed line in Fig. 1). When scintillations are low-pass filtered by the MASS apertures (i.e. normal indices), the mismatch at high frequencies does not matter, and a good model of the scintillation index results (see below).

Multiple layers cross-modulate each other. I checked that the spatial power spectrum of the logarithm of intensity can be well modeled by the sum of the individual layers. However, the spatial filtering by the MASS apertures is applied to the intensity, not to its logarithm. Hence, the cross-modulation appears. It is accounted for empirically because our corrections use the measured indices from all layers combined.

2 MASS simulation

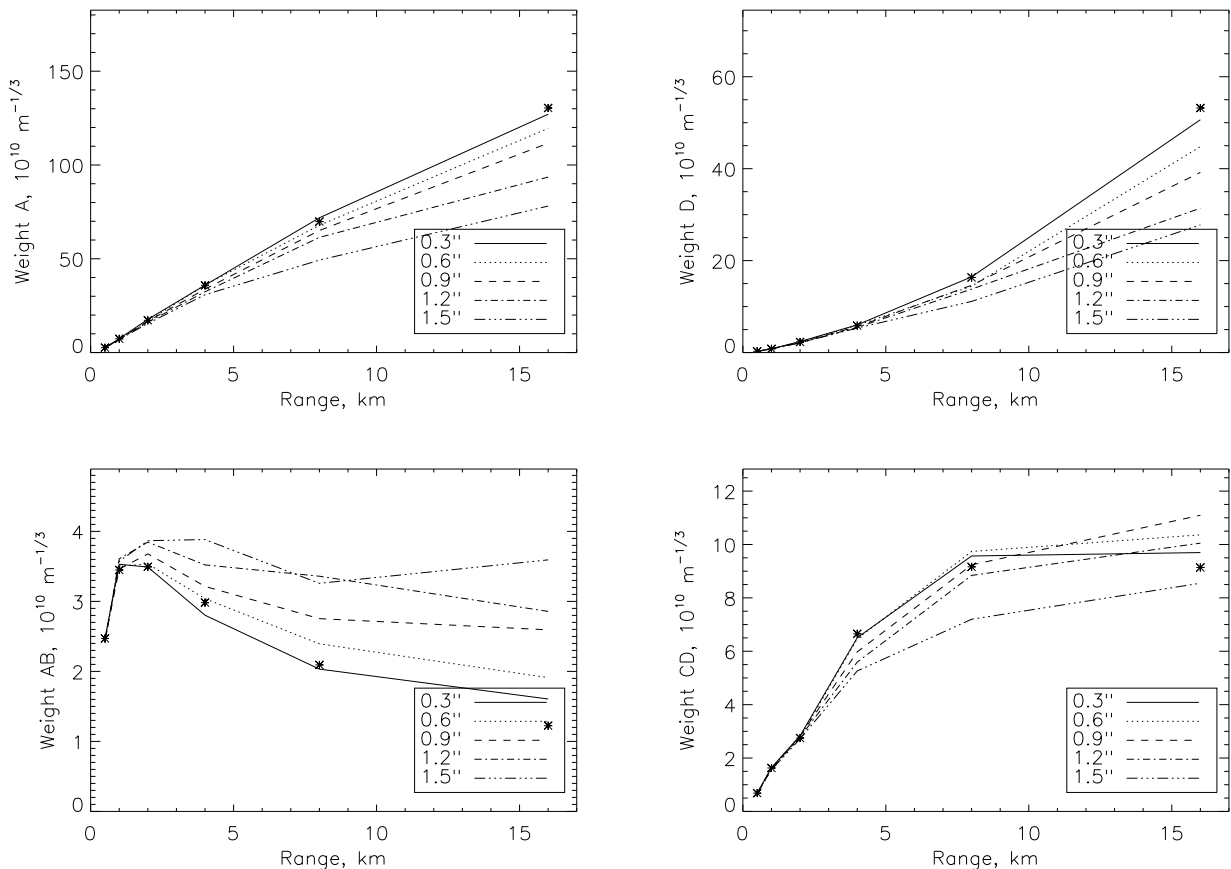


Figure 2: Weighting functions for selected normal (top row) and differential (bottom row) indices in the MASS apertures as determined from the simulations (run3). The approximate theoretical WFs are plotted as asterisks.

Several simulation runs have been done to determine realistic scintillation indices as would be measured by MASS. Previously (in 2004), similar simulations were performed for monochromatic light. Now we model polychromatic scintillation with `simatmpoly.pro`. The spectrum of the light was represented by 3 wavelengths with equal weight, mimicking roughly the MASS response. The theoretical polychromatic weights have been computed only approximately, for an average wavelength of 467nm and a quasi-Gaussian bandwidth of 100nm. The parameters common to all simulations are listed below. The physical size of simulated phase screens and intensity patterns is 2.56m across, with 2.5mm pixels.

```
lambda = [0.4,0.45,0.55]*1.e-6
sp = [1.,1.,1.]/3.
ngrid = 512
pixel = 0.0025
d = [1.9,3.15,5.6,8.0]*0.01 ; aperture diameter, m: Meade
```

In the previous simulations, the intensity patterns have been “trailed” across MASS apertures, simulating both spatial and temporal response. This time, we simply computed the spatial filters corresponding to the MASS apertures and applied them to the power spectra of the intensity fluctuations. Two alternative programs of index calculation were used, both in `indcalc.pro`. The first, “slow” option directly multiplies the 2D power spectrum of intensity fluctuations by the 2D aperture filter functions. The second (actually used) routine first calculated the radially averaged power spectrum, and only then makes products and integration over the radius in 1D. We checked that the simulations and the index calculations closely reproduce theory for weak scintillation.

The first run, `run3a.pro`, simulates a single turbulent layer placed at “standard” MASS altitudes 0.5, 1, 2,...16km, and with varying total integral (seeing).

The second run `run4.pro` simulates 2 layers at 10km and 2km. The high layer contains 10%, 50%, or 90% of turbulence: `profs=[[0.1,0.9],[0.5,0.5],[0.9,0.1]]`. In both runs the seeing takes values `see = [0.3,0.6,0.9,1.2,1.5]` arcseconds.

The third run `run5.pro` is similar to the run4, except that the altitudes of the two layers are 8km and 1km, with 4 profiles simulated, `profs=[[0.1,0.9],[0.3,0.7],[0.5,0.5],[0.7,0.3]]`

Figure 2 shows the simulation results for the run3 interpreted in terms of weighting functions (WFs). Under strong scintillation, all WFs for the normal indices become smaller, i.e. saturate. The behavior of the differential WFs is more complex. The WFs AB and AC always increase, but the AD at first decreases, especially for low altitudes. The remaining 3 differential WFs BC,BD, and CD also demonstrate this non-monotonous behavior. This can be traced to the shape of the intensity spectrum (Fig. 1) which decreases at low frequencies but increases at high frequencies, in comparison with the weak-scintillation theory.

3 Modeling

3.1 Stretching and scaling

We have a guidance for modeling the scintillation indices from the previous studies and from experience. In case of strong scintillation, the MASS restoration is always done with consistently small residuals. It means that the measured set of indices can be well modeled by the classical weak-scintillations WFs. Of course, the results of these models are wrong: the restored profiles shift to

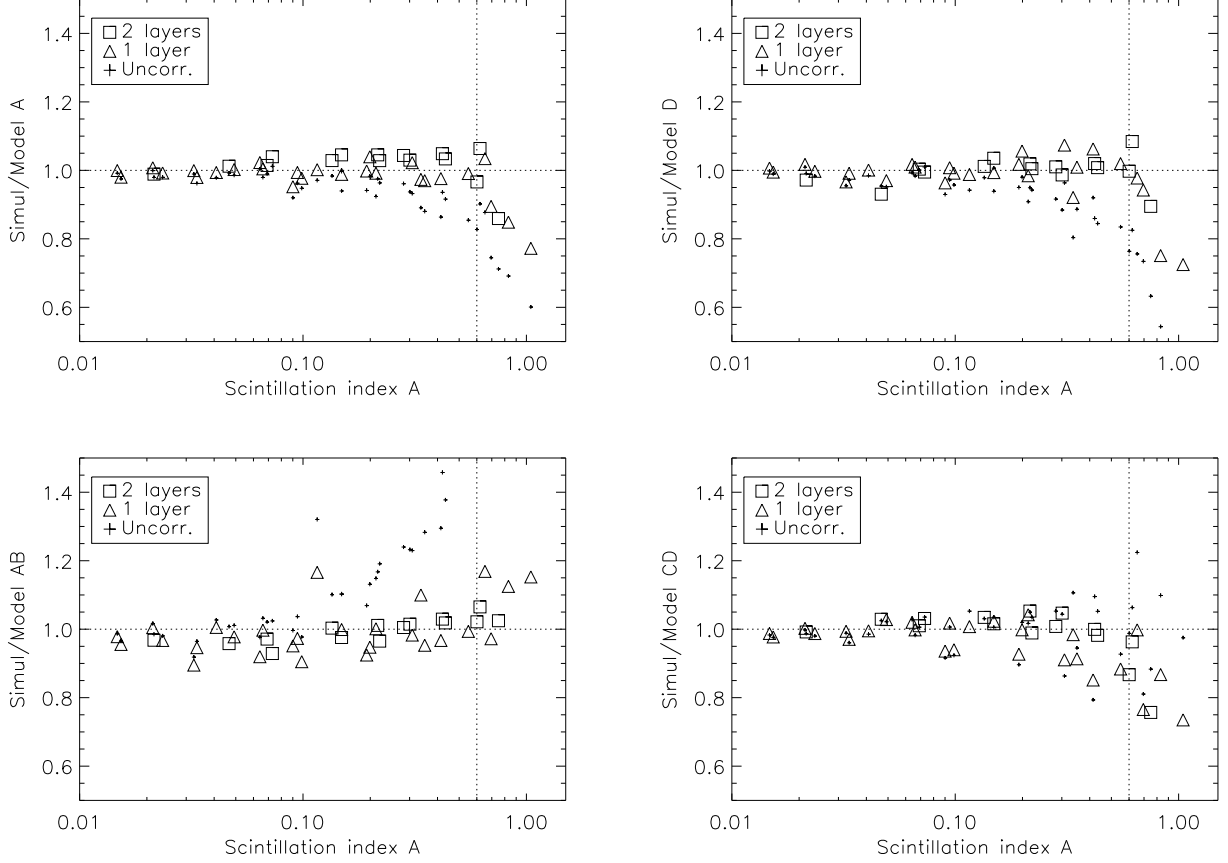


Figure 3: Ratio of measured to modeled scintillation indices for run3 and run4, with a stretch-and-scale correction. Selected normal (top row) and differential (bottom row) indices in the MASS apertures as determined from the simulations are divided by the linear model (small crosses) or by the corrected model (empty symbols).

lower altitudes, and the turbulence strength is over-estimated. This over-estimation (“overshoot”) of turbulence integral is well described by the $1 + 0.7A$ factor, where A is the index in the A-aperture. The recipe for the model emerges from these considerations.

Normal scintillation indices under moderate scintillation can be modeled by the same weighting functions, but with reduced altitudes. Denoting by A the index in the smallest aperture A, the altitude reduction is approximately $1 + 0.3A$. The modified weight is then

$$W_A^*(z) = W_A \left(\frac{z}{1 + 0.3A} \right). \quad (1)$$

The same altitude reduction factor works well for other normal indices B,C, and D.

To model the differential indices, we keep the same altitude reduction factor and increase the WF by some amount (individual for each aperture pair) to compensate for the excess of high frequencies. For AB, for example, the model will be

Table 1: Bias and variance of scintillation indices (percent). Altitude stretch 1+0.3A.

Index	Raw		Corrected		Factor
	Aver.	rms	Aver.	rms	
A	93.6	4.0	101.4	2.7	1
B	90.2	5.3	99.1	3.1	1
C	89.6	6.6	99.5	3.5	1
D	91.7	5.4	101.2	3.3	1
AB	125.1	14.3	100.3	5.4	1 + 1.0A
AC	111.0	9.1	98.1	3.1	1 + 0.9B
AD	102.0	8.4	98.3	3.8	1 + 0.9B
BC	107.2	9.8	98.0	3.6	1 + 0.7B
BD	99.7	8.8	97.7	4.5	1 + 0.7C
CD	100.1	8.1	98.1	5.8	1 + 0.7C

$$W_{AB}^*(z) = (1 + 1.0A) W_{AB} \left(\frac{z}{1 + 0.3A} \right). \quad (2)$$

For AC, AD, BC, BD and CD, the only thing that changes is the coefficient in the brackets. Instead of 1.0A, we put, respectively, 0.9B, 0.9B, 0.7B, 0.7C, and 0.7C. The code is `r3c.pro` for the run3, and `r4c.pro` for the run4. The code `r34c.pro` analyzes the results of both runs jointly. Note that in the results presented here, the theoretical weights are approximated by a quasi-Gaussian spectral response. Exact weight calculation for given spectrum has been implemented later (code `wcalc2.pro`), and the fitting results change slightly. The numerical values for the coefficients correspond to the exact weights.

The comparison of old (linear) and new models with the simulations is given in Fig. 3. Clearly, the proposed correction removes most of the “saturation” from the normal indices and most of the “overshoot” from the differential ones. This empirical correction, however, only works at moderate scintillation. The vertical line in Fig. 3 depicts the index A=0.6 that can be considered as a limit of the empirical model.

In order to quantify the quality of the correction, we analyzed jointly the results of both runs in the range of scintillation index A from 0.1 to 0.6 (18 different combinations of profile and seeing satisfy this condition). At lower scintillation, the correction becomes small (and unnecessary), and at stronger scintillation the model breaks apart.

Table 1 compares the bias and scatter (around the mean) of the ratio of measured-to-modeled indices, in percent. It can be seen that most of the bias is removed and, more importantly, the scatter of indices is reduced significantly, to a level of 3-4%. It appears in Fig. 3 that the indices for the single-layer case show somewhat larger scatter, and this can be confirmed by a separate analysis of the runs. Moreover, the parameters of the model (coefficients and altitude stretch factors) can be optimized separately for each run. For example, using the altitude stretch of 1+0.4A, we can reach the rms of nearly 1% for the results of the run3, but this approximation is worse for the run4.

3.2 Linear correction

Let S be the 10-element vector of measured scintillation indices, S_0 – the vector of theoretical indices expected in the linear theory without saturation, and S^* – vector of corrected indices. A rather general correction formula can be written as

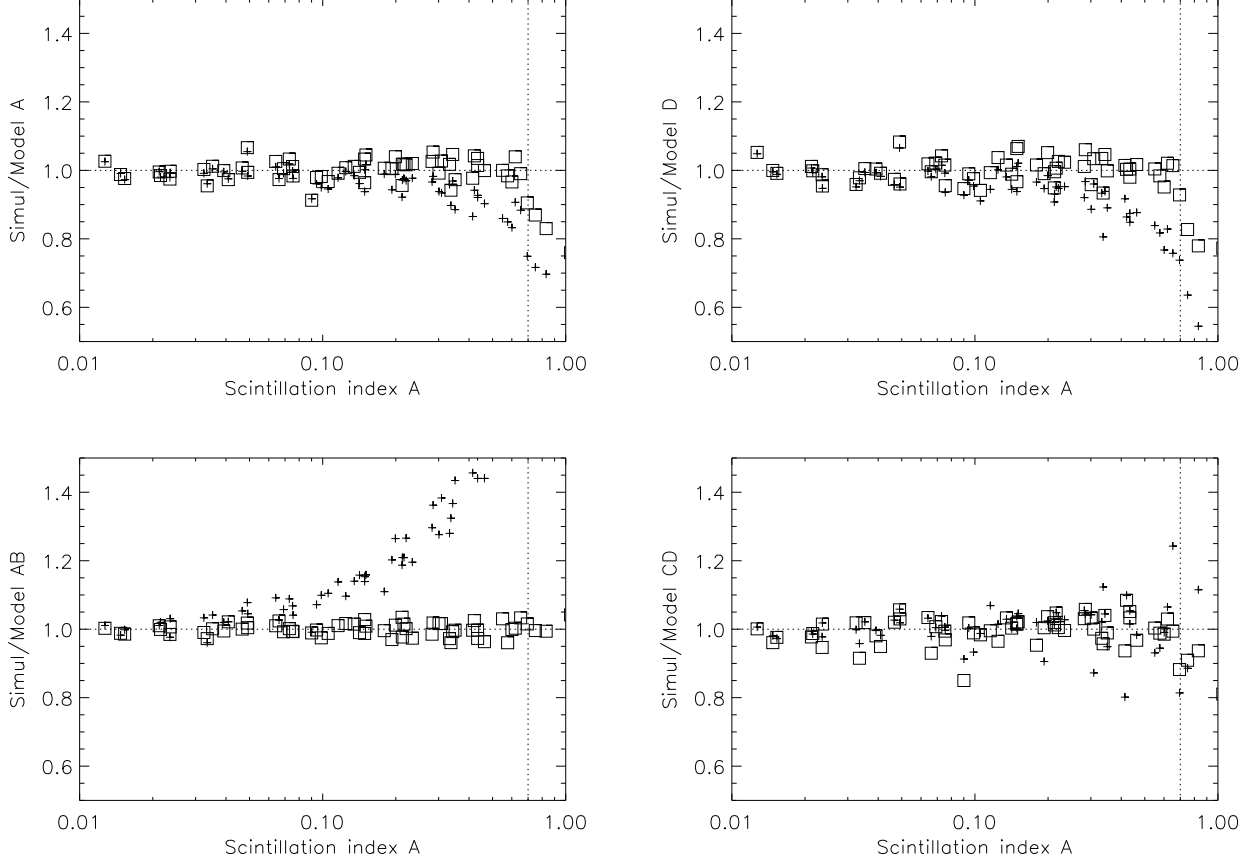


Figure 4: Ratio of measured to modeled scintillation indices for runs 3, 4, 5. Selected normal (top row) and differential (bottom row) indices in the MASS apertures as determined from the simulations are divided by the weak-scintillation model without correction (crosses) or after correcting by Eq. 3 (empty squares).

$$S^* = \frac{S}{1 + ZS} \approx S_0. \quad (3)$$

The rationale for selecting this formula is that it automatically removes corrections for weak scintillation, and that this type of formula works already for the differential indices. Here, Z is a 10×10 correction matrix.

The idea is to determine Z from the results of simulations, by least squares (LS) fitting. This matrix is “learned” from simulations. The LS problem can be re-written as

$$ZS = Y, \quad Y = S/S_0 - 1. \quad (4)$$

The “learning” is restricted to the relevant range of scintillation indices, A from 0.1 to 0.7, because weak scintillation does not need correction (but adds statistical noise), whereas strong scintillation is hopeless. Thus, a total of K simulations are selected with $0.1 < A < 0.7$ (either from a single run, e.g.

r4d.pro, or from the merged runs 3,4,5 – code r5dd.pro). The right-hand matrix Y has dimension $10 \times K$, same as S . The standard LS solution is

$$Z = (SS^T)^{-1}(S^TY) \quad (5)$$

The theoretical indices are computed accurately with wtcalc2.pro. The inversion of the normal matrix (SS^T) is done by SVD, selecting singular values above 1e-3 of the maximum. The finally adopted correction matrix Z (all runs, $K = 35$ relevant simulations) is

A	B	C	D	AB	AC	AD	BC	BD	CD
-0.010	-0.107	0.098	0.102	0.230	0.349	-0.268	0.041	-0.302	-0.042
-0.037	-0.121	0.115	0.117	0.241	0.339	-0.353	0.031	-0.362	-0.054
-0.102	-0.240	0.024	0.067	0.293	0.480	-0.271	0.068	-0.347	-0.050
-0.175	-0.152	-0.171	-0.114	-0.054	-0.058	0.088	-0.001	0.077	0.004
0.324	0.615	0.023	-0.100	-0.631	-1.034	0.596	-0.146	0.760	0.114
0.394	0.685	0.393	0.185	-0.384	-0.839	-0.142	-0.183	0.164	0.018
0.374	0.402	0.596	0.410	0.182	0.057	-0.711	-0.065	-0.524	-0.075
0.408	0.597	0.514	0.302	-0.146	-0.479	-0.422	-0.141	-0.149	-0.025
0.371	0.321	0.654	0.475	0.347	0.320	-0.869	-0.029	-0.720	-0.101
0.400	-0.012	0.756	0.633	0.947	1.395	-1.133	0.155	-1.239	-0.156

For example, the denominator in Eq. 3 for the index A will be $1 - 0.010A - 0.107B + 0.098C + \dots$

We see that the coefficients of Z take moderate values, hence there will be no noise amplification in the corrected indices. The threshold in the SVD influences the Z matrix, of course: lower thresholds lead to larger coefficients and to better modeling of the indices. However, with only 35 cases and 10 free parameters to model each index, we have only 25 degrees of freedom. By setting a too low SVD threshold, we model part of the simulation statistical noise. By trial and error it is determined that a threshold of 1e-3 is the best choice.

The application of formula (3) to the joint data set of 3 runs results in the complete elimination of the index bias (not surprisingly) and in the reduction of the scatter. The Table below shows uncorrected and corrected values for average ratios of indices to model, and the rms values of these ratios in the relevant range $0.1 < A < 0.7$.

	Uncorrected	Corrected		Uncorrected	Corrected
A	0.961	0.061	1.010	0.033	
B	0.930	0.082	1.008	0.032	
C	0.909	0.099	1.000	0.036	
D	0.935	0.083	1.005	0.046	
AB	1.248	0.223	0.996	0.016	
AC	1.152	0.147	1.001	0.019	
AD	1.062	0.063	1.010	0.026	
BC	1.120	0.113	1.007	0.025	
BD	1.037	0.047	1.011	0.027	
CD	1.019	0.036	1.008	0.034	

The best correction is for the index AB, rms 1.6%, and the worst correction – for D, rms 4.6%. The results are illustrated in Fig. 4.

4 Application to profile restoration

Both “stretch-and-scale” and linear approaches were applied to the runs 4 and 5 in order to see how they improve the quality of profile restoration. The results are rather similar. Here, only the linear correction is discussed.

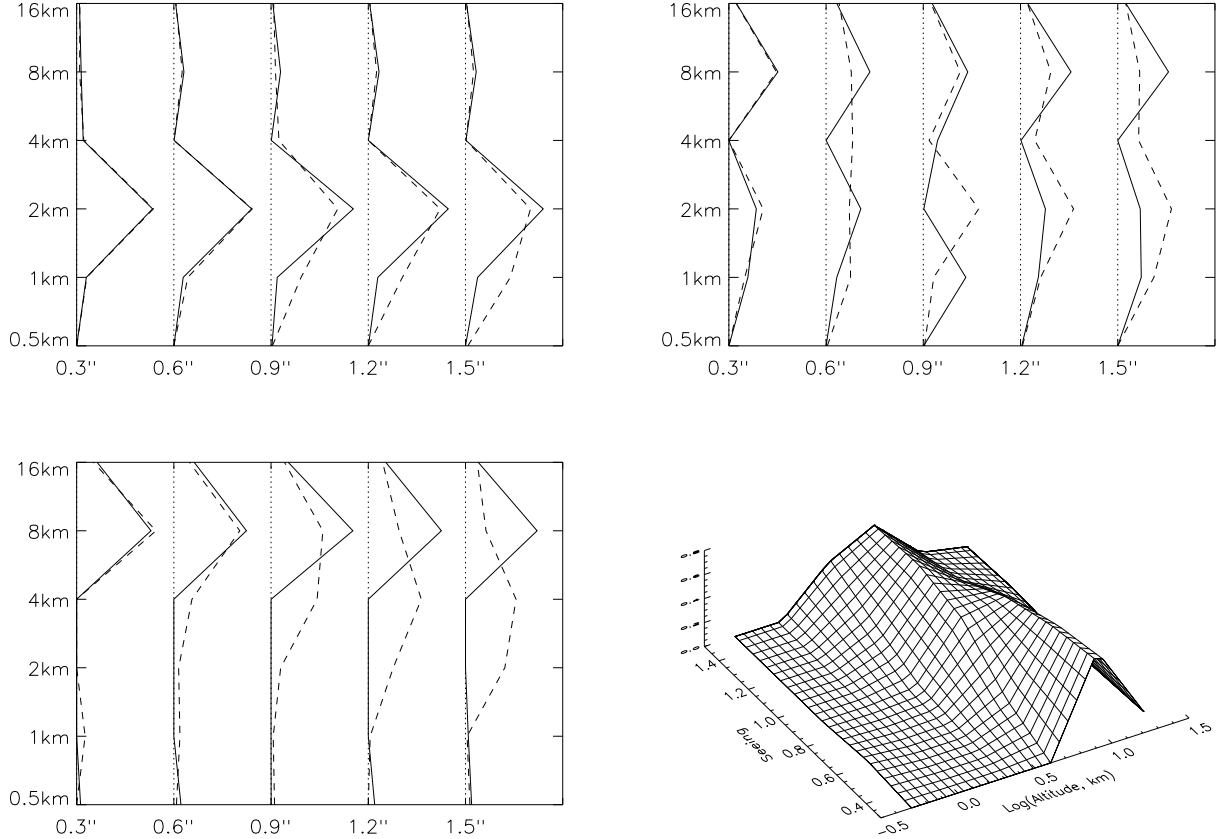


Figure 5: Restorations of turbulence profiles in the run 4 without correction (dashed lines) and with correction (full lines), for the 3 profiles and different seeing values. The 10-km layer contains 10%, 50% and 90% of turbulence, respectively. The 3D plot illustrates the altitude shift in the restored profile without correction for the last profile.

The profiles restored in the run 4 with and without correction are plotted in Fig. 5. When the bulk of turbulence is concentrated at 2 km, the scintillation is weak and the correction does not change the profiles. However, when a strong layer at high altitude dominates, the profiles without correction are significantly biased towards low altitude. At the same time, both seeing and isoplanatic angle are over-estimated (Fig. 6). The correction removes these biases. We note, however, that the restored profiles are not perfect even with correction, especially at low altitudes where the restoration algorithm can re-distribute turbulence to lower altitudes. The input indices in these simulations contain statistical noise of few percent, hence this is a realistic test of the restoration procedure and its accuracy.

Similar tests for the run 5 are plotted in Fig. 7 and Fig. 8. The programs used to process and plot

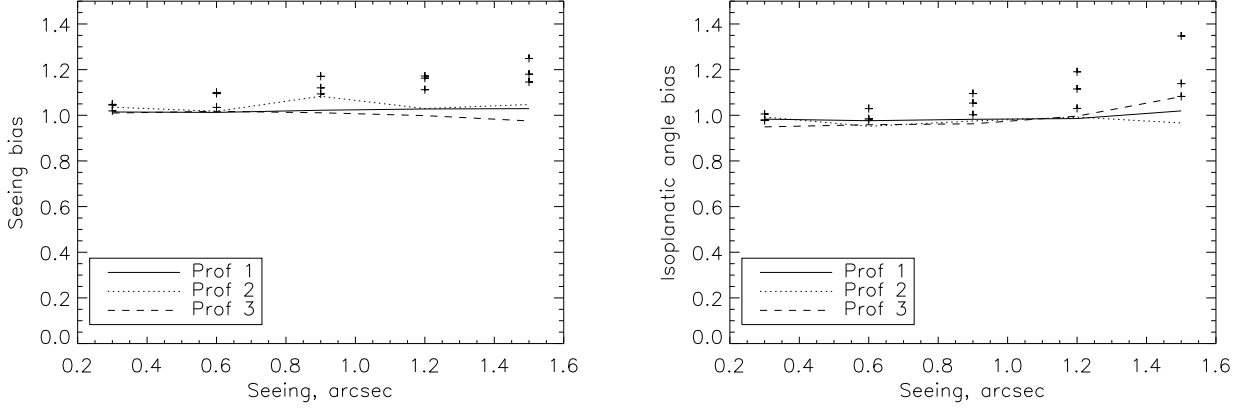


Figure 6: Ratio of seeing (left) and isoplanatic angle (right) calculated from the restored profiles to the true values (run 4). Crosses indicate the data without index correction.

the runs are `run4rest.pro` and `run5rest.pro`.

5 Conclusions

In the absence of accurate analytic description of the scintillation spatial spectrum under realistic condition of moderately strong scintillation, the simple empirical approach proposed here seems reasonable. It makes a good job in correcting the saturation effects to the first order. The bias can be virtually eliminated with the linear correction, and the residual rms scatter of 2-3% comes mostly from the statistical noise of the simulations.

Both approaches (linear and stretch-scale) improve the profile restoration. The correction removes biases in the measured seeing (“overshoots”) and isoplanatic angles. These biases, however, are quite small even before correction. The new procedure leads to a more faithful profile reconstruction, preventing the “leak” of turbulence to lower altitudes under moderately strong scintillation. Finally, when the scintillation index in the A-aperture exceeds 0.7, the results of MASS should be considered as unreliable or tentative.

The proposed correction is empirical. The coefficients depend on the adopted instrument parameters such as wavelength, spectral response and aperture diameters. A test run 5a with aperture diameters increased by 1.3 times has been done. The results are yet to be discussed.

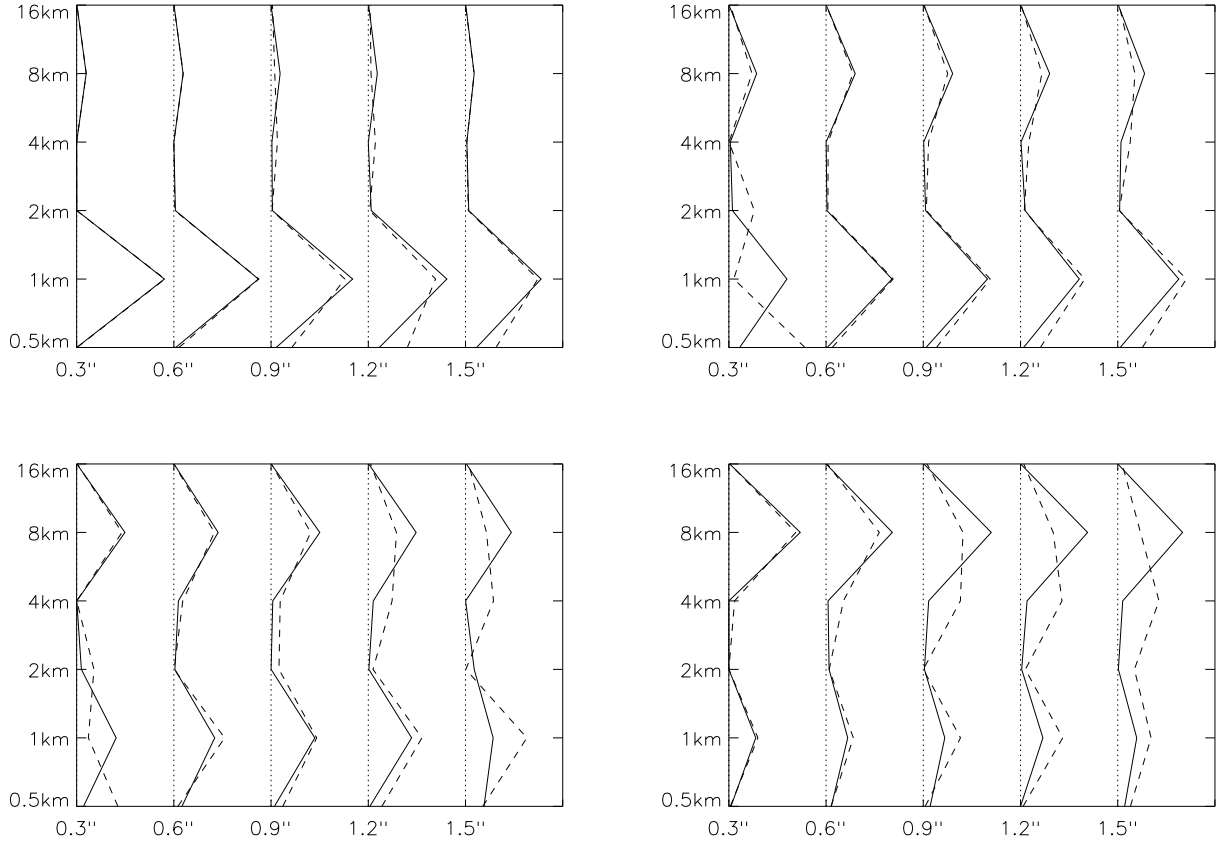


Figure 7: Restorations of turbulence profiles in the run 5 without correction (dashed lines) and with correction (full lines), for the 4 profiles and different seeing values. The fraction of turbulence in the 8km layer is 0.1, 0.3, 0.5, and 0.7. The lower layer is at 1km.

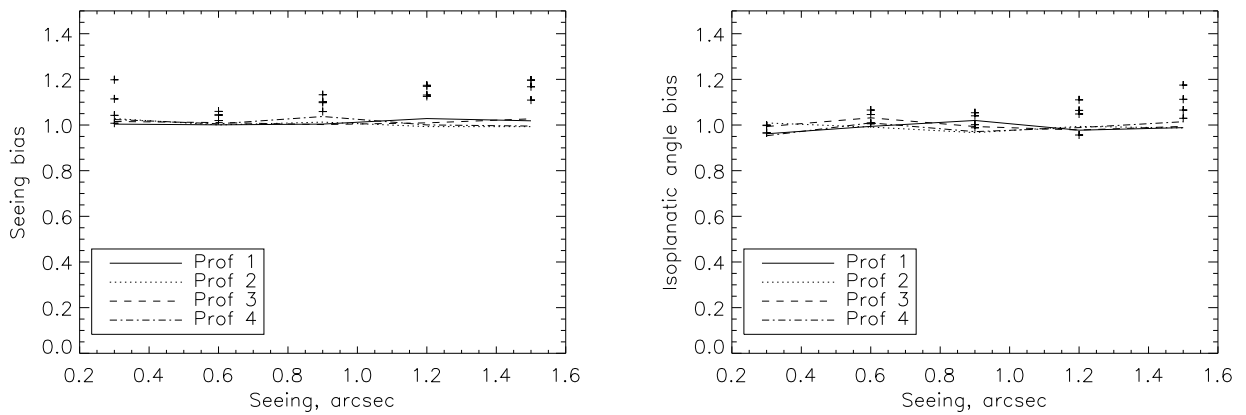


Figure 8: Ratio of seeing (left) and isoplanatic angle (right) calculated from the restored profiles to the true values (run 5). Crosses indicate the data without index correction.